Force microscope using a fiber-optic displacement sensor

D. Rugar, H. J. Mamin, R. Erlandsson,[a] J. E. Stern, and B. D. Terris

IBM Research Division, Almaden Research Center, 650 Harry Road, San Jose, California 95120-6099

(Received 1 June 1988; accepted for publication 27 July 1988)

A force microscope is described which uses a fiber-optic interferometer as the cantilever displacement sensor. Low thermal drift and reduced susceptibility to laser frequency variation are achieved due to the small (several micrometer) size of the interferometer cavity. A sensitivity of 1.7×10^{-4} Å/$\sqrt{\text{Hz}}$ is observed for frequencies above 2 kHz. The drift rate of the sensor is on the order of 3 Å/min. As an initial demonstration, laser-written magnetic domains in a thin film sample of TbFeCo were imaged.

INTRODUCTION

The atomic force microscope (AFM) was introduced by Binnig, Quate, and Gerber[1] as a method for high-resolution topographic imaging of both insulators and conductors. The AFM consists of a sharp tip which interacts with the sample and a cantilever which converts the force acting on the tip into a displacement. In the original design, the cantilever displacement was measured using a tunneling probe. Alternative displacement measurement schemes have also been used, including optical[2–4] and capacitive[5] techniques.

The advantages of optical techniques for measuring cantilever deflection have been discussed previously.[2,3,6] The heterodyne interferometer used by Martin *et al.*[3] achieves excellent sensitivity and provides immunity to optical path variation when used for ac displacement measurements. This mode of operation, where the lever is driven near its resonant frequency, is useful for measuring van der Waals, magnetic, and electrostatic forces. Another widely used imaging mode for force microscopy simply monitors instantaneous lever deflection when the tip is in repulsive contact with the sample.[1,7–9] Depending on scanning speed, this mode can require measurements with frequency response at or near dc. Heterodyne interferometers can be used for dc displacement measurements, but have no special immunity to optical path-length drift when used in this way. The interferometer used by McClelland *et al.*[2] and Erlandsson *et al.*[6] has fewer signal processing components compared to heterodyne interferometers and is capable of both ac and dc measurements. This scheme is susceptible to thermal drift and laser frequency variation, however, since the reference mirror and the cantilever are separated by a distance of several centimeters. The ideal displacement sensor would be suited to both ac and dc measurements and have high sensitivity, large dynamic range, and good dc stability.

This paper describes a new force microscope implementation which is based on the fiber-optic interferometer previously described by Drake and Leiner.[10] It has high sensitivity for both ac and dc measurements and exhibits low drift due to the small size of the interferometer cavity. The sensor part of the instrument is simple and compact and, because of the fiber-optic implementation, should be suitable for operating in remote environments, such as in ultrahigh vacuum or at low temperatures.

I. FORCE MICROSCOPE DESIGN

Figure 1 shows the basic design of the instrument. It consists of a high-stability helium-neon laser[11] ($\lambda = 633$ nm) which generates a collimated optical beam approximately 1 mm in diameter. The beam passes through a Faraday isolator, a $3\times$ beam expander, and a half-wave plate. The Faraday isolator (Hoya Electronics, model M-500) serves to isolate the laser from retroreflected light, which can adversely affect the stability of the laser. The half-wave plate orients the polarization horizontally before the beam passes through the polarizing beam splitter. The light is focused onto the core region of a single-mode optical fiber using a $10\times$ objective lens. A glass cover slip is located just in front of the fiber and a drop of optical microscope immersion oil (or other index matching fluid) fills the gap between the fiber and the cover slip. This arrangement places the air-glass interface out of focus so that any reflected light is uncollimated, thereby reducing spurious interference effects related to this interface.

The fiber carries the light along its 4-μm-diam core to the mechanical components of the force microscope. Located along the fiber path is a 360° fiber loop which, by virtue of the strain induced birefringence, serves as the fiber equivalent of a quarter-wave plate.[12] The fiber is terminated with a perpendicular cleaved facet which is positioned close to the cantilever of the force microscope. The fiber-to-cantilever spacing is on the order of 10 μm or less.

Approximately 4% of the light propagating down the fiber is reflected by the glass-air interface at the end of the fiber. This interface serves as the reference reflector in the interferometer and the reflected light serves as a reference beam. The other 96% of the light exits the fiber and spreads by diffraction with a characteristic angle determined by the numerical aperture (NA) of the fiber (6° for a 0.1 NA fiber). This light impinges on the cantilever of the force microscope and a fraction of the light is scattered back into the fiber. The fraction of the light that reenters the fiber core is determined, in part, by the fiber-cantilever spacing. The total optical power propagating back through the fiber is determined by the interference between the two reflected components.

The backward propagating light in the fiber makes a second pass through the fiber loop. It then exits the fiber and is recollimated by the objective lens. The radius of the fiber

 © 1988 American Institute of Physics

Downloaded 05 Sep 2009 to 131.152.36.108. Redistribution subject to AIP license or copyright; see http://rsi.aip.org/rsi/copyright.jsp

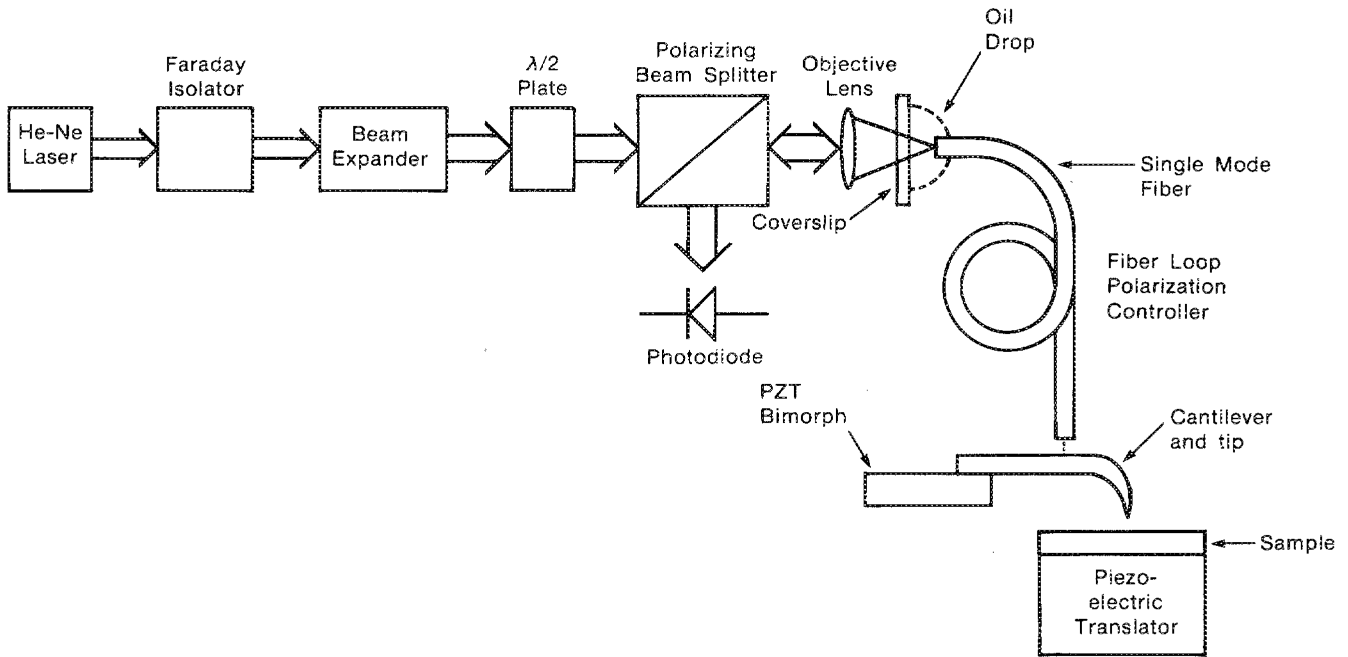

FIG. 1. Force microscope using fiber-optic interferometer sensor.

loop and the angle of the plane of the loop are chosen so that the light is vertically polarized when it exits the fiber. For the fiber used in our apparatus (Newport F-SV), a loop radius of 2 cm gave good results. The vertically polarized light is reflected by the polarizing beam splitter and focused onto a photodiode detector.

The optical and mechanical portions of the microscope are constructed on a small (60×60 cm) optical breadboard. The breadboard is suspended by elastic latex tubes for vibration isolation. A plastic enclosure covers the instrument to reduce the effects of air currents and acoustic noise.

II. MICROSCOPE SENSITIVITY

If the effects of multiple reflections in the interferometer cavity are ignored, then the interferometer response can be analyzed simply as the two component interference between the reflections from the fiber end and the cantilever. For maximum sensitivity, we assume that the phases of the two reflections are adjusted to be in quadrature (i.e., relative phase shift of $\pi/2$). For a cantilever oscillating sinusoidally at frequency ω with amplitude much less than a wavelength, the optical power on the detector is given by

$$P_{\rm det} = P_{\rm av} + P_{\rm sig} \sin \omega t, \qquad (1)$$

where $P_{\rm av}$ is the average power at the detector and $P_{\rm sig}$ is the amplitude of the optical power oscillation due to the oscillating cantilever. $P_{\rm av}$ and $P_{\rm sig}$ are given by

$$P_{\rm av} = P_{\rm inc}(R_f + R_c) \qquad (2)$$

and

$$P_{\rm sig} = P_{\rm inc}(8\pi/\lambda)(R_f R_c)^{1/2}\sqrt{2}A_{\rm rms}, \qquad (3)$$

where $P_{\rm inc}$ is the optical power incident at the end of the fiber, R_f and R_c are the effective reflectivities from the fiber end and cantilever, respectively, and $A_{\rm rms}$ is the root mean square (rms) amplitude of the cantilever oscillation. When $R_c = R_f$, which can be achieved by adjusting the fiber-cantilever spacing, the fringe visibility is unity and Eq. (3) can be written as

$$P_{\rm sig} = P_{\rm av}(4\pi/\lambda)\sqrt{2}A_{\rm rms}. \qquad (4)$$

The detector photocurrent is $SP_{\rm det}$, where S is the detector responsivity (A/W). The rms shot noise current associated with the photocurrent is given by

$$i_{\rm shot} = (2eSP_{\rm av}\Delta f)^{1/2}, \qquad (5)$$

where e is electronic charge and Δf is the detection bandwidth. The shot noise mimics cantilever motion and sets a fundamental limit on interferometer sensitivity. The ratio of rms signal to rms shot noise is unity when $SP_{\rm sig}/\sqrt{2} = i_{\rm shot}$. Using Eqs. (4) and (5), this gives a rms equivalent noise amplitude of

$$A_{\rm noise} = (e\Delta f/2SP_{\rm av})^{1/2}(\lambda/2\pi). \qquad (6)$$

For our instrument, $P_{\rm av} = 47\ \mu$W, $S = 0.4$ A/W, and $\lambda = 633$ nm, which yield a rms equivalent noise amplitude of 7×10^{-5} Å/$\sqrt{\rm Hz}$.

In a test of the sensitivity of our instrument, the interferometer noise was evaluated for a tungsten tip mounted in the microscope, but with no sample present. Figure 2 shows the noise spectrum of the interferometer as measured with a spectrum analyzer for frequencies up to 10 kHz. At low frequencies, below 2 kHz, laser noise and noise due to spurious mechanical vibration is dominant. With the exception of the two peaks near 5 kHz, which are due to two thermally driven cantilever resonances, the noise floor above 2 kHz is nearly flat and has a spectral density of approximately 1.7×10^{-4} Å/$\sqrt{\rm Hz}$. This is within a factor of 2.5 of the shot noise limit. The excess noise is due to Johnson noise, laser noise, and the fact that the fringe visibility was less than unity ($R_f \neq R_c$).

Downloaded 05 Sep 2009 to 131.152.36.108. Redistribution subject to AIP license or copyright; see http://rsi.aip.org/rsi/copyright.jsp

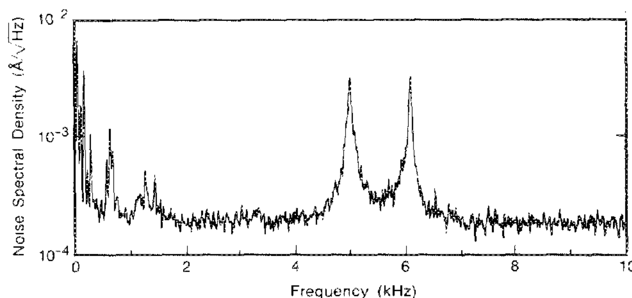

FIG. 2. Noise spectrum of the force microscope for tungsten wire cantilever with thermally excited resonances near 5 kHz.

Figure 3 shows the interferometer output when the cantilever is driven sinusoidally at resonance (5 kHz) with a 0.3-Å peak-to-peak amplitude. The electronic bandpass with 1–10 kHz and a high signal-to-noise ratio is obvious.

When the force microscope is used for profilometry in the repulsive mode, low noise for frequencies near dc is important. In this regime, laser power fluctuation and low-frequency phase variation of spurious interfering reflections are the primary noise sources. The total rms noise was measured to be 0.01 Å rms in a 100–1000 Hz bandpass and 0.3 Å rms in a 0.3–3000 Hz bandpass. In an air conditioned laboratory room with no special temperature control, the drift rate was on the order of 3 Å/min.

III. APPLICATION TO MAGNETIC FORCE MICROSCOPY

One growing application of force microscopy is the imaging of domain structures in magnetic materials.[13,14] The force microscope described above has been successfully used for imaging domains in a 2000-Å-thick film of an amorphous TbFeCo alloy. The film was sputtered deposited onto a glass substrate and had an easy axis of magnetization perpendicular to the film plane. The saturation magnetization of the film was approximately 80 emu/cm^3 and the coercivity was 6.2 kOe. A domain pattern was thermomagnetically written in the film using a laser beam.

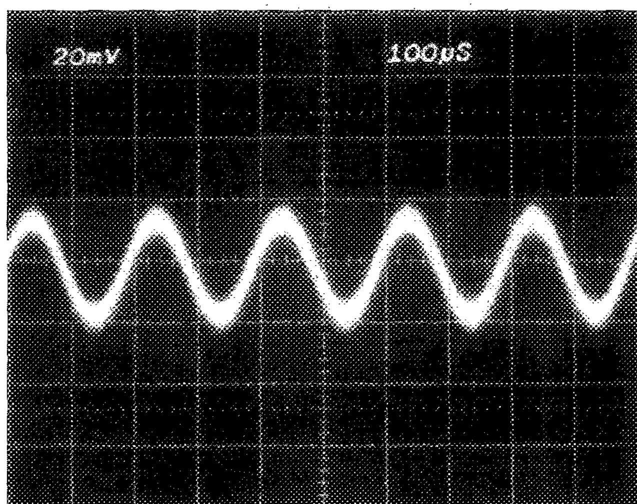

FIG. 3. Oscilloscope trace from interferometer when cantilever is driven with a 0.3-Å peak-to-peak amplitude.

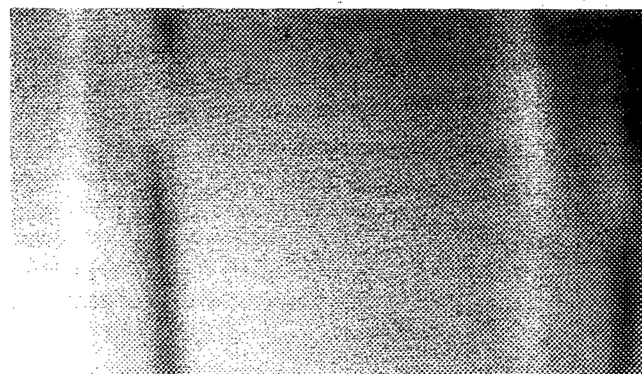

FIG. 4. Magnetic force image of two stripe-like domains in a TbFeCo thin film. Arrows point to locations of domain walls, which can produce either attractive (bright) or repulsive (dark) force gradients. The distance between closely spaced arrows is approximately 7 μm.

The tip/cantilever consisted of an electrochemically etched iron wire approximately 550 μm in length with no bend. The wire had a tapered geometry with a base diameter of 15 μm and a resonant frequency of 43 kHz. The angle between the tip and sample was approximately 15°.

The principles of magnetic force microscopy using ac detection have been described previously.[14,15] Briefly, a magnetic tip/cantilever is driven near resonance with an amplitude, in our case, on the order of 50 Å. The presence of a force gradient from the sample acts to shift the resonant frequency of the cantilever and, thereby, change the amplitude of oscillation. The tip-to-sample spacing is servo-controlled using a piezoelectric positioner to maintain constant force gradient as the sample is scanned transversely in a two-dimensional raster scan. The image is a map of the servo-control signal as a function of position. Approximately 15 min were required to scan an image with 50 scan lines.

In our experiments, three forces are acting on the tip: magnetic, electrostatic, and van der Waals. The electrostatic force is due to a voltage applied to the sample and serves to provide a convenient, controllable force for maintaining servo-lock.

Figure 4 shows a magnetic force image of two laser written stripes. The two stripes are regions where the perpendicular magnetization in the sample has reversed orientation. The locations of domain walls are marked with arrows. Note that for each stripe, one domain wall is bright and the other is dark. The bright wall corresponds to a region of greater attractive force gradient, while the dark wall corresponds to a region of repulsive magnetic force gradient. Note that the force gradient exerted by the interior of the stripe appears to be equivalent to the force gradient exerted by the background magnetization.

The observed contrast is consistent with the expected magnetic force distribution. For a magnetic thin film with perpendicular magnetization, the magnetic field outside of the film is expected to be zero except in the vicinity of domain walls. Thus the central region of a wide domain stripe

Downloaded 05 Sep 2009 to 131.152.36.108. Redistribution subject to AIP license or copyright; see http://rsi.aip.org/rsi/copyright.jsp

should look equivalent to the space between stripes. This characteristic is evident in Fig. 4. The left and right walls of the written stripe appear to produce opposite force gradients. This is consistent with the expected behavior[16] if the dominant component of the force is $m_x \partial B_x / \partial z$, where m_x is the component of the effective magnetic moment of the tip perpendicular to the domain wall (parallel to the sample) and B_x is the parallel component of induction resulting from the domain wall.

ACKNOWLEDGMENTS

The authors thank C.-J. Lin for the TbFeCo sample and D. W. Abraham, S. Chiang, G. Hadziioannou, C. M. Mate, G. M. McClelland, and H. K. Wickramasinghe for helpful discussions.

[a] Present address: Dept. of Physics and Measurement Technology, Linkoping University, S-581 83 Linkoping, Sweden.

[1]G. Binnig, C. F. Quate, and Ch. Gerber, Phys. Rev. Lett. **56**, 930 (1986).
[2]G. M. McClelland, R. Erlandsson, and S. Chiang, *Review of Progress in Quantitative Nondestructive Evaluation*, edited by D. O. Thompson and D. E. Chimenti (Plenum, New York, 1987), Vol. 6B, p. 1307.
[3]Y. Martin, C. C. Williams, and H. K. Wickramasinghe, J. Appl. Phys. **61**, 4723 (1987).
[4]N. M. Amer and G. Meyer, Bull. Am. Phys. Soc. **33**, 319 (1988).
[5]G. M. McClelland (personal communication).
[6]R. Erlandsson, G. M. McClelland, C. M. Mate, and S. Chiang, J. Vac. Sci. Technol. A **6**, 266 (1988).
[7]G. Binnig, Ch. Gerber, E. Stoll, T. R. Albrecht, and C. F. Quate, Europhys. Lett. **3**, 1281 (1987).
[8]T. R. Albrecht and C. F. Quate, J. Appl. Phys. **62**, 2599 (1987).
[9]O. Marti, B. Drake, and P. K. Hansma, Appl. Phys. Lett. **51**, 484 (1987).
[10]A. D. Drake and D. C. Leiner, Rev. Sci. Instrum. **55**, 162 (1984).
[11]Laboratory For Science, model 210.
[12]H. C. Lefevre, Electron. Lett. **16**, 778 (1980).
[13]J. J. Saenz, N. Garcia, P. Grutter, E. Meyer, H. Heinzelmann, R. Wiesendanger, L. Rosenthaler, H. R. Hidber, and H.-J. Guntherodt, J. Appl. Phys. **62**, 4293 (1987).
[14]Y. Martin, D. Rugar, and H. K. Wickramasinghe, Appl. Phys. Lett. **52**, 244 (1988).
[15]Y. Martin and H. K. Wickramasinghe, Appl. Phys. Lett. **50**, 1455 (1987).
[16]H. J. Mamin, D. Rugar, J. E. Stern, and B. D. Terris (unpublished data).

Downloaded 05 Sep 2009 to 131.152.36.108. Redistribution subject to AIP license or copyright; see http://rsi.aip.org/rsi/copyright.jsp